

# Influence of the Phases Stabilization on Corrosion Behavior of Novel Ti-10Mo-xZr Alloys for Bio-implants Applications

Alaa Keshitta<sup>1\*</sup>, Ahmed H. Awad<sup>2</sup>, Hayam A. Aly<sup>3</sup>, Gamal Abd ELnaser<sup>1</sup>, Tharwat Elsarag<sup>1</sup>, Shaban Abdou<sup>1</sup>.

<sup>1</sup> Department of Production Engineering and Mechanical Design, Faculty of Engineering, Port Said University, Port Said 42526, Egypt

<sup>2</sup> Design and Production Department, Faculty of Engineering Ain Shams University, Cairo 11535, Egypt.

<sup>3</sup> Central Metallurgical Research and Development Institute (CMRDI), Helwan 11421, Egypt.

\*Corresponding author: E-mail: [alaa.keshitta@eng.psu.edu.eg](mailto:alaa.keshitta@eng.psu.edu.eg) (Alaa Keshitta)

Received .....17 April 2025

Accepted .....26 April 2025

Published .....30 June 2025

## Abstract

Newly designed titanium alloys composed of vital elements are being researched to represent alternatives to commercial alloys. Ti-10Mo alloy with different Zr additions was investigated through corrosion tests in saline media. All studied alloys are in the  $\alpha+\beta$  region designed using the d-orbital method after applying the equivalent Mo ( $[Mo]_{eq}$ ) concentrations equation. The microstructure analysis approved the appearance of  $\alpha$ - laths and  $\beta$ - grains with varied percentages measured from XRD diffraction. The  $\beta$  phase amount in the studied alloys is inversely proportional to the corrosion rate.  $\beta$  phase percentages are 94.6%, 47.5 % and 82.3%, opposed to corrosion rates of  $0.95451 \times 10^{-3}$ ,  $1.7819 \times 10^{-3}$ , and  $1.0288 \times 10^{-3}$  mm/year for (Ti-10Mo, Ti-10Mo-3Zr, and Ti-10Mo-6Zr) alloys, respectively. Large difference between phases induces potential variation, causing micro galvanic cells to result in high corrosion as achieved in Ti-10Mo-3Zr alloy. Zr addition forms a protective layer over implant material, that significantly affected the electrochemical properties of Ti-10Mo-6Zr alloy.

**Keywords:** Titanium alloys, Bio-implants, Corrosion, Phase stability, Microstructural analysis.

## 1. Introduction

Titanium and its alloys have proved to attain better mechanical properties than stainless steel and Co-Cr alloys; it has been determined that these materials are most frequently employed as implants. The titanium alloy most utilized in biomedical applications is Ti-6Al-4V, with good corrosion resistance [1][2]. Nonetheless, studies have shown that aluminum and vanadium can both result in neurological problems and hypersensitive reactions to human tissues [3][4].

Due to its exceptional mechanical qualities, excellent corrosion resistance, and superior biocompatibility, titanium (Ti) finds employment in a variety of industrial sectors, including biomedical, petrochemical, automotive, and aerospace [5][6]. Ti alloys are extensively utilized in biomedical applications, including bone plates, pacemakers,

prosthetic knee and hip joints, orthopedic and dental implants, and screws for fixing fractures [7][8].

Corrosion is a natural phenomenon that follows the second law of thermodynamics. This law states that a particular system tends to achieve more excellent thermodynamic stability. Corrosion is irreversible; either a chemical or electrochemical reaction happens when metal and the environment are in contact [9]. Corrosion behavior can be investigated through various electrochemical methods to judge the amount of metal corroded inside the corrosive medium. The electrochemical techniques can mainly classified into open circuit potential, potentiodynamic polarization, and electrochemical impedance spectroscopy [10].

According to the galvanic metal series, titanium cannot be counted as intrinsically noble as it has a

standard potential value equal to -1.63 V. Despite titanium behavior in most environments, it shows high corrosion resistance. This resistance, which approaches nobility in most environments, mainly refers to the passive layer formed onto a titanium metal surface and causes passivation and protection towards surroundings. This behavior achieved chemical stability in titanium alloys, making it a great candidate for corrosion resistance applications, including the biomedical field [11].

It has been discovered that commercial Ti-6Al-4V, an  $\alpha+\beta$  titanium alloy, has adverse effects because of its reduced biocompatibility brought on by specific alloying components. These substances can potentially cause health problems by releasing ions into the bloodstream. Further worries are raised by the possibility of material escaping from the implant and entering the surrounding tissues. Debris and ions have both been linked to an increased risk of diseases such as metabolic bone abnormalities and Alzheimer's disease [3].

The two equilibrium phases that make up titanium alloys are  $\alpha$  and  $\beta$ ; alloying elements are used to determine whether these phases stabilize. Three classes of these elements are distinguished as neutral,  $\beta$ -stabilizing, and  $\alpha$ -stabilizing elements [12].  $\beta$  type Titanium alloys, including non-toxic elements such as Nb, Mo, Zr, Ga, Sn, and Ta, are the safest for bio-implants; these elements improve biocompatibility, mechanical properties, wear, and corrosion resistance [13][14][15][16][17][18]. The oxide layer is formed upon specific physiological conditions over the metal surface; this layer is physiochemically affected by the bulk material chemical composition plus solution chemistry [19].

Previous work claimed that Ti-Zr alloys released lower ions than pure Ti; thus, the formed ZrO<sub>2</sub> layer achieved higher stability than TiO<sub>2</sub>, so the Zr addition to Ti element is expected to improve the corrosion resistance [20]. Pinghua et al. [21] achieved higher cytocompatibility through the investigated Ti-Zr alloy rather than CP Ti, and these promising results present Zr as a favorable alloying element with Ti as a candidate for bio-implant applications. Previous work found that Zr element addition to Ti-10Mo alloy reduced magnetic susceptibilities, representing a paramagnetic property suitable during MRI examination [22].

This work investigates new V-free Ti-alloys as alternatives to commercial Ti-6Al-4V alloy. The vanadium toxic influence makes researchers go beyond this element with newly designed alloys seeking close

mechanical properties to Ti-6Al-4V alloy but better biocompatibility. The stability of the phases affects the corrosion resistance of bio-implants, which is the scope of the current work. The newly designed alloys are non-allergenic, free of toxic elements and paramagnetic materials, have high corrosion resistance and good mechanical properties, and are accepted as cost-effective.

## 2. Experimental Procedures

### 2.1 Alloy design:

Previous studies investigated biomedical Ti-Mo alloys as a candidate for new vanadium-free bio-implants and achieved promising results. This work is an extension of earlier studies focusing on the effect of Zr element addition to Ti-10Mo alloy after applying thermo-mechanical treatment using hot forging. Superior research work on modified alloying systems targets more investigation on the impact of  $\beta$  plus  $\alpha$  phases stability by altering the percentages of Zr element addition. The compositions investigated are Ti-10Mo-xZr, where x has values of 0, 3, and 6 wt%; these alloys are named after TMZ0, TMZ3, and TMZ6, respectively.

From empirical approaches, the values of the  $\overline{e/a}$  and  $\Delta\overline{r}$  of can represent the kind of deformation occurring in the alloys. Where  $\overline{e/a}$  is (average electron-to-atom ratio) and  $\Delta\overline{r}$  is (atomic radius difference).  $\overline{e/a} - \Delta\overline{r}$  Graphs illustrate the estimated twinning/stress-induced region as well as the slipping region. Also  $\overline{Bo} - \overline{Md}$  diagram could approach the material deformable behavior by obtaining both  $\overline{Bo}$  (the covalent bond strength between Ti and other alloying elements) and  $\overline{Md}$  (the correlation with the electronegativity and the metallic radius of alloying elements). This is called the d-electron method and applies a relation between the amount of stabilized  $\beta$  phase and plastic deformation behavior; the  $\overline{Bo} - \overline{Md}$  diagram shows the boundaries separating the phase stabilization between  $\beta$ ,  $\beta+\alpha''$ ,  $\beta+\alpha$ ,  $\alpha$ .

Overall stability assessment of both  $\alpha$  and  $\beta$  phases can be conducted by studying each alloying element's impact, namely Mo-equivalent ([Mo]<sub>eq</sub>). concentrations. [Mo] equation provided below represents each element-specific contribution:  $(\text{Mo}_{\text{eq}})_Q = 1.0 \text{ Mo} + 1.25 \text{ V} + 0.59 \text{ W} + 0.28 \text{ Nb} + 0.22 \text{ Ta} + 1.93 \text{ Fe} + 1.84 \text{ Cr} + 1.51 \text{ Cu} + 2.46 \text{ Ni} + 2.67 \text{ Co} + 2.26 \text{ Mn} + 0.30 \text{ Sn} + 0.47 \text{ Zr} + 3.01 \text{ Si} - 1.47 \text{ Al}$  (wt pct). [23]

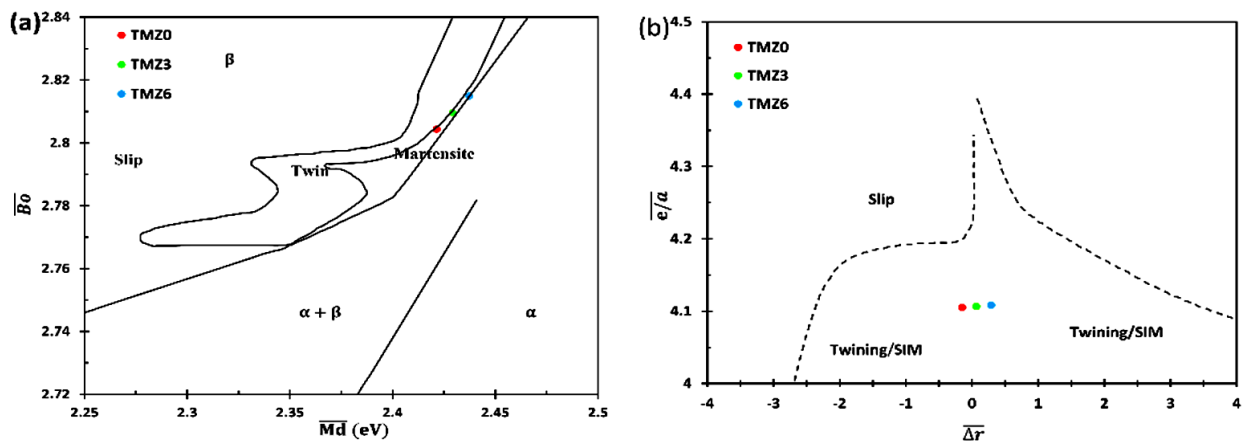


**Fig. 1** : Boundaries of expected deformation mechanisms obtained for (TMZ0, TMZ3, and TMZ6) alloys[24].

**Table 1.** Different values of the current alloys studied.

	$\overline{Md}$ (eV)	$\overline{Bo}$	$\overline{e/a}$	$\overline{\Delta r}$	Moecq
TMZ0	2.421	2.804	4.105	-0.147	0.1
TMZ3	2.429	2.810	4.107	0.069	0.1141
TMZ6	2.437	2.815	4.108	0.293	0.1282

## 2.2 Material preparations

Titanium, molybdenum, and zirconium, raw materials with high purity of up to 99.99%, were applied to the ultrasonic cleaning device after being immersed in both distilled water and high-purity ethanol for 15 minutes each time. Each element was weighed with a digital balance with accuracy up to the third digit. The materials were produced using an electric arc furnace and melting media, which included argon inert gas. Each sample was flipped twice and remelted, seeking high homogeneity; the final ingot was around 100 g.

Three ingots were produced using the arc furnace with compositions in wt%: Ti-10Mo, Ti-10Mo-3Zr, and Ti-10Mo-6Zr. All the ingots were applied to the homogenization treatment in which all samples were placed in a muffle furnace at a temperature above  $\beta$ -transus (900° C) for 30 minutes. Then, all ingots were applied to hot forging processing and quenched in water.

## 2.3 Material examination

### Microstructural analysis

Specimens were cut for microstructure examinations using a wire-cutting machine; each sample dimension

is (10mm\*10mm\*8mm). All samples were applied to the grinding desk wheels and polished with sandpaper with grades starting with 180 grits and up to 4000 grits. Colloidal silica suspension is used to polish samples up to the mirror surface, followed by using Kroll etchant. The optical microscope model (ZEISS AXIO Imager Alm device) was used for observing the microstructure. X-ray crystallography (Shimadzu -6100) is used for phase detection with a range from 30° to 90°; the diffraction is used to calculate entire phase percentages.

### Corrosion behavior

To determine the corrosion behavior of Ti-10Mo-xZr alloys, electrochemical testing was performed using a standard three-electrode setup connected to an AUTOLab PGSTAT 30 potentiostat. Platinum foil served as the counter electrode, a saturated calomel served as the reference electrode, and the Ti-10Mo-xZr alloy served as the working electrode.

The samples were examined in saline media; the saline was prepared in the laboratory with a composition of 9 gm/liter of sodium chloride (NaCl) salt dissolved in distilled water.

### 3. Results and Discussions

#### 3.1. Microstructure Analysis

The micrographs show the stabilized phases in all studied alloys, which are presented in Figure 2. All alloys included both  $\beta$  grains and  $\alpha$  laths; the percentage of each phase varied as presented; these results agree with  $\overline{Bo} - \overline{Md}$  calculations in which all designed alloys are located in the  $\alpha + \beta$  region, as shown in Figure 1. Shear bands appeared through the grains, which are generated by the effect of hot forging. Elmay et al.

discussed the deformation stress effect on  $\beta$  phase stability, which initiated the formation of another allotropic phase [25].

Previous work on Ti-7.5Mo-xZr alloys studied solution treatment effects related to  $\beta$  phase formation, which was suppressed upon thermal treatment [26]. Correa et al. investigated the influence of Zr and Mo elements added to Ti-alloys; both elements provided  $\beta$  phase stabilization [27]. The thermomechanical treatments and amount of Zr addition have different influences on the phase stabilizations, as concluded by the previous studies.

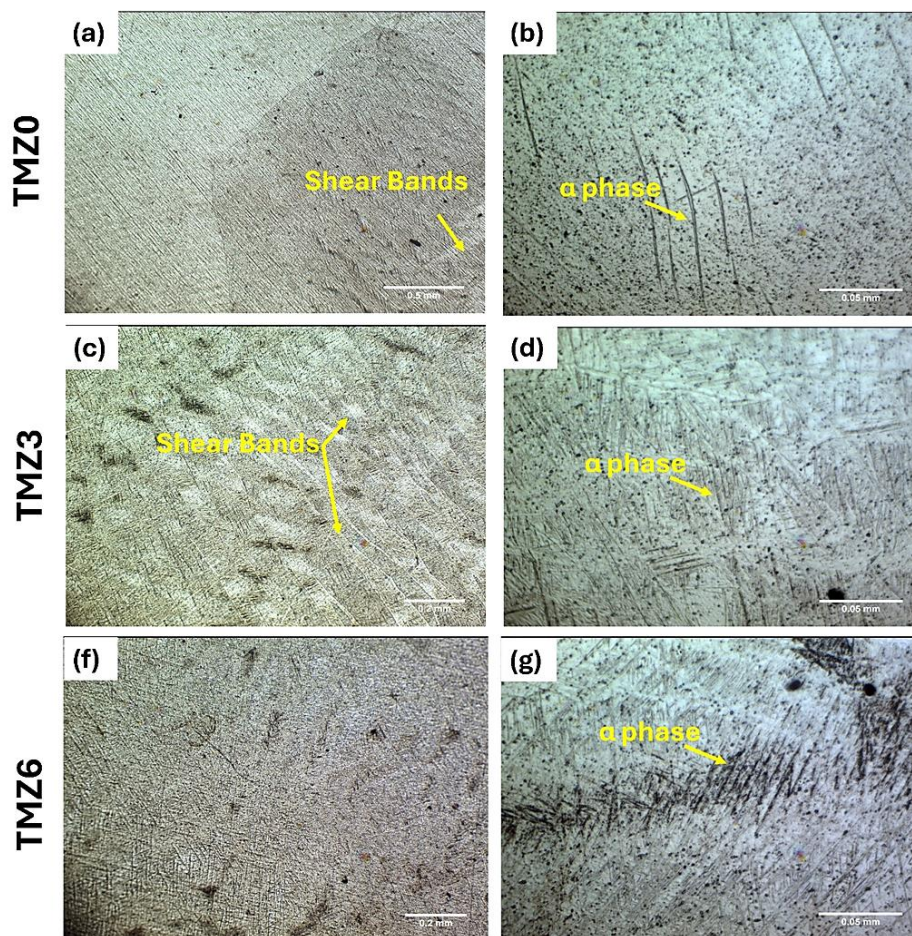


Fig. 2 Microstructural optical micrographs for TMZ0, TMZ3, and TMZ6 alloys.

The phase percentages in hot forged TMZ0, TMZ3, and TMZ6 alloys are presented in Figure 3. The XRD test was used for the calculation of the phase percentages, the card numbers (PDF 01-086-2610) were used to detect the  $\beta$  phase, and (PDF 01-077-3481, PDF 01-077-3484) were used for plotting the  $\alpha$  phase.  $\beta$  phase is the predominant phase in both TMZ0

and TMZ6 alloys, with weight percentages equal to 94.6% and 82.3%, respectively. TMZ3 alloy exhibited a higher  $\alpha$  phase amount with a value of 52.5%. The dual effect of the influence of thermo-mechanical treatment and Zr element addition achieved the differences in stabilized phases.

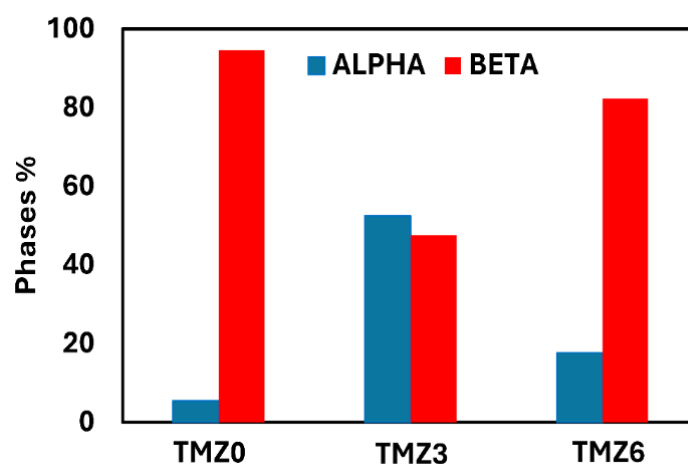


Fig. 3 Phases percentages in TMZ0, TMZ3, and TMZ6 alloys.

### 3.2 Corrosion analysis

The corrosion behavior for Ti-10Mo-xZr alloys with varying percentages of Zr element addition and phase stabilized amounts was studied through saline media at room temperature. The alloying components, microstructure, phase quantity, production methods, and porosity influence corrosion behavior [28]. The corrosion results are summarized and listed in Table 2. All the tested alloys displayed a closed activation-controlled manner through the cathodic zone; the entire linear polarization and electrochemical impedance spectroscopy (EIS) curves are plotted in Figure 4.

Linear polarization is presented in Figure 4(a), in which the passive behavior was achieved as no pitting occurred on tested sample surfaces. Rapid potential increase was exhibited in all alloys at -100, -130, and -160 mV for TMZ0, TMZ3, and TMZ6 alloys, respectively. The formation of a more stable and compact Zr oxide coating on the surface may be linked to the increased corrosion resistance resulting from adding Zr [29][30].

According to the authors, stable passivation coatings and abilities were formed as the corrosion rate decreased [31]. From the literature, the micro galvanic cell produced by the potential difference between the local corrosion potentials of the dual phases had a lower current when the proportion of the  $\alpha$  phase was less [32]. The Tafel slope is used to obtain both corrosion potential ( $E_{corr}$ ) and corrosion current density ( $i_{corr}$ ). The lowest  $i_{corr}$  was achieved in TMZ0 alloy with a value of  $0.0976 \times 10^{-6}$  A/cm<sup>2</sup>; TMZ0 exhibits the highest obtained corrosion resistance with the lowest CR value equal to  $0.95451 \times 10^{-3}$  mm/year.

The dual effect of the Zr addition and phases stabilized percentages with contrast influence explains the non-linear behavior achieved.

EIS charts are shown in Fig. 4. The Nyquist plot is presented in Figure 4 (b), which shows the formation of a passive and protective layer that has the same shape and an incomplete semicircle arc in all the cases that were studied. The bigger diameter of the TMZ0 alloy compared to the other alloys indicates more favorable corrosion resistance behavior. The phase shift and Bode plot along the frequency range are displayed in Figure 4 (c, d). All the alloys under examination demonstrated capacitive behavior for the passive along the frequency range from 0.1 to 100 Hz. It is possible to implant the alloys in a negative-sloped straight line. For TMZ0 alloy, however, the same trend was seen; for instance, the alloy line had a greater negative slope than the TMZ3 alloy line. For TMZ0, TMZ3, and TMZ6 alloys, the phase angle is near -76, -62, and -61°, respectively. From previous work, with a very stable passive film over the surface, the phase angle was 90° for pure capacitive behavior [33]. The phase angle, where both resistive and capacitive responses coexist, was below the levels discussed above. In all cases, the phase angle approaches zero at frequencies ( $\log F$ ) greater than 10<sup>4</sup> Hz, resulting in the impedance plateau and electrolyte resistance.

Phase stability and corrosion resistance under the chemical composition conditions were enhanced by the Mo and Zr additions in the current work. The amount of  $\beta$  phase decreased to 47.5% with the addition of 3 wt% Zr, as opposed to 94.6% and 82.3% with 0 wt% Zr and 6 wt% Zr, respectively. Additionally, by creating a more consistent, stable, and protective MoO<sub>3</sub> layer on

the corrosive surface, the addition of Mo improved the corrosion resistance.  $\text{TiO}_2$ ,  $\text{MoO}_3$ , and  $\text{ZrO}_2$  made up the passive layers on the corrosive surface [34]. Previous work discussed the effect of oxide on the implant texture with different corrosion parameters;

thus, rough surface texture enhanced implant adaptation with bone [35, 36]. The current findings also agree with another study that investigated the corrosion behavior of Ti-Mo-Zr alloys in saline media and discussed the effect of Zr and Mo additions [37].

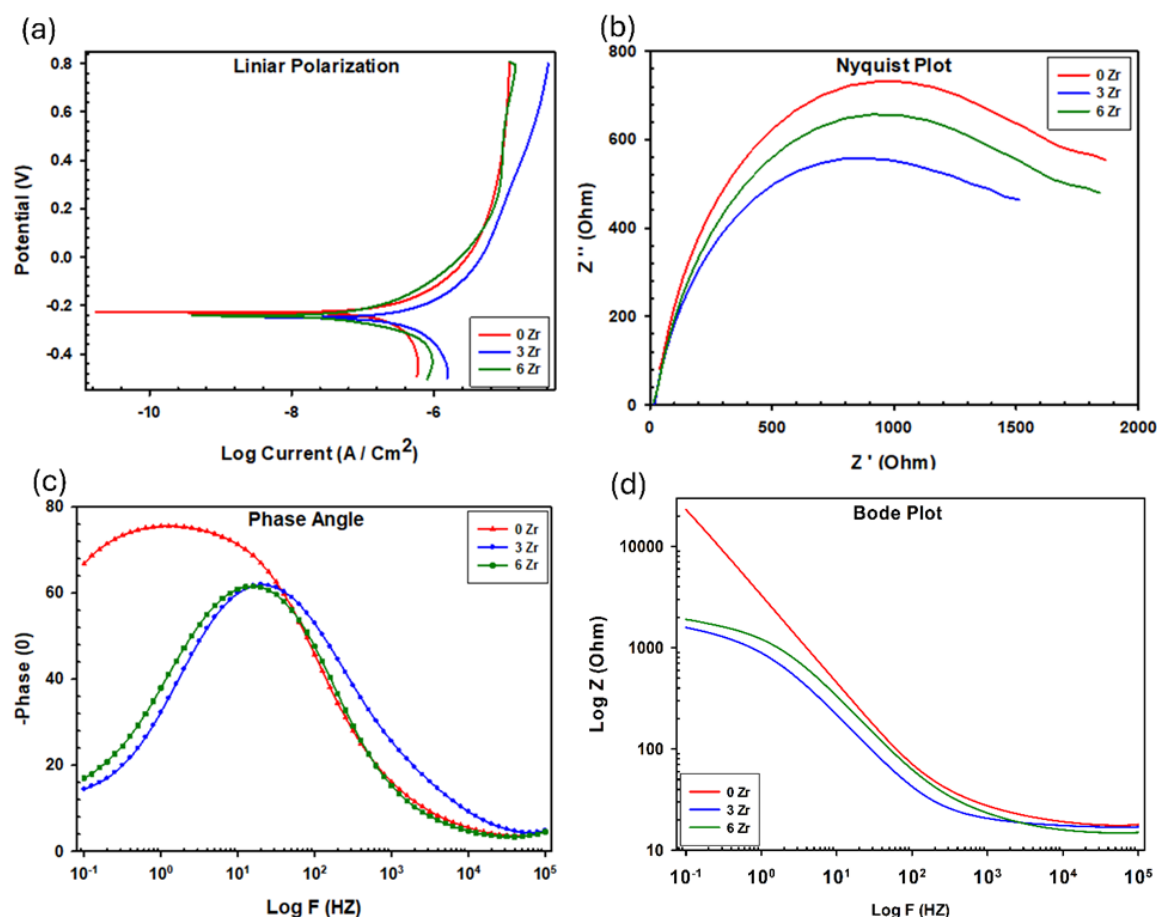


**Fig. 4** (a) Potentiodynamic polarization, (b) Nyquist plot, (c) Phase angle, (d) Bode plot of hot forged TMZ0, TMZ3, and TMZ6 alloys.

The Randles circuit, which is shown as an inset in Fig. 5, is used to match the EIS spectra to better analyze the physical behavior. Table 2 contains the results of the electrochemical testing. The electrolyte, polarization resistance, constant phase element, and ideal factors are presented by the electrical parameters, which are  $R_s$ ,  $R_p$ ,  $Q$ , and  $n$ , respectively. For the conditions under study, the  $R_s$  of the saline alloys that were tested fell within a narrow range of 19.22 to 21.36  $\Omega$ . The passive layer's capacitance in the 0.78–0.84 n range was found to be less than optimum ( $n < 1$ ). The  $R_p$  is associated chiefly with corrosion resistance and is inversely proportional to  $i_{\text{corr}}$  and corrosion rate (CR). With an  $R_p$  of about 1881.7  $\Omega$ , the results showed that

the TMZ0 alloy had the best corrosion resistance. The TMZ3 alloy, in contrast, showed the lowest  $R_p$  of about 970.08  $\Omega$ , which consists of the highest  $i_{\text{corr}}$  determined by the potentiodynamic tests.

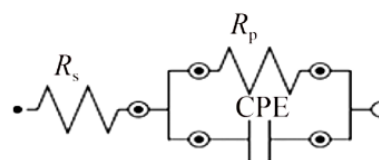


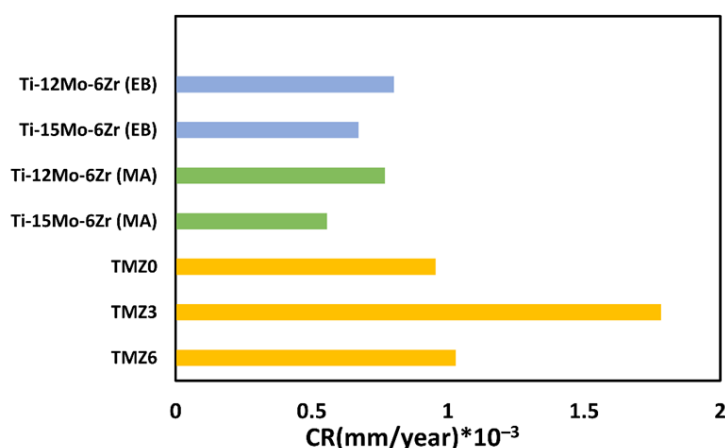
**Fig. 5** Randles circuit of TMZ0, TMZ3, and TMZ6 alloys

**Table 1:** Electrochemical parameters of hot forged TMZ0, TMZ3, and TMZ6 alloys

Alloy	E <sub>corr</sub> (mV/cm <sup>2</sup> )	i <sub>corr</sub> (A/cm <sup>2</sup> ) *10 <sup>-6</sup>	R <sub>s</sub> (Ω)	R <sub>p</sub> (Ω)	N	Q (μMho *SN)	CR(mm/year)*10 <sup>-3</sup>
TMZ0	-3.703	0.0976	19.22	1881.7	0.78734	73.5	0.95451
TMZ3	-3.706	0.1776	19.473	970.08	0.84044	99.9	1.7819
TMZ6	-3.549	0.1007	21.36	1683.9	0.82014	67.8	1.0288

The corrosion rate findings obtained from the current work are compared with the outcomes of the previous paper in Figure 6. Prior work investigated the corrosion rate of Ti-12Mo-6Zr and Ti-15Mo-6Zr alloys through different manufacturing processes, which are elemental blend (EB) and mechanical alloying (MA) [37]. The effect of Mo element addition to Ti-Mo-Zr alloys on the phase stability showed that Mo addition stabilized the β phase. Molybdenum (Mo) element was proved to lower β-transus temperature in Ti-alloys acting as β stabilizer element [13][38].

For both techniques, Mo element addition in Ti-15Mo-6Zr alloy showed a higher β amount than Ti-12Mo-6Zr alloy. Subsequently, Ti-15Mo-6Zr alloy achieved a lower corrosion rate than Ti-12Mo-6Zr alloy for both (EB) and (MA) techniques. These findings agree with the current study as the corrosion rate is inversely proportional to β phase amount. From Figure 6, TMZ0 alloy has the lowest corrosion rate among current work with a value of  $0.95451 \times 10^{-3}$  mm/year; also, TMZ0 has the highest β phase percentage, equal to 94.6%.

**Fig. 6** Corrosion rate of Ti-Mo-Zr alloys compared to previous studies [37].

## Conclusions

This study discussed the effect of stabilized phases on corrosion behavior for novel Ti-10Mo-xZr, as X=0, 3, 6 wt%. The following are the outputs;

1. The improvement in beta stability in this study is responsible for the improvement in corrosion resistance. Besides, the alloys with a more significant fraction of β phase have better corrosion properties; for example, the CR of TMZ0 alloy is  $0.95451 \times 10^{-3}$  mm/year, and the CR of TMZ3 alloy is  $1.7819 \times 10^{-3}$  mm/year. This is

because the fractions of the β phase are more prominent, at 94.6% and 47.5%, respectively.

2. Thermo-mechanical treatment, as well as Zr addition to Ti-10Mo, were the factors affecting the phase stabilization behavior.
3. The lowest Corrosion rate was achieved in TMZ0 alloy, as the predominant phase is β and the highest percentage in all studied alloys as β phase has more resistance to corrosion.
4. The corrosion rate of TMZ3 alloy was the maximum value achieved in this study, as the high α percentage causes a localized galvanic cell that initiates the corrosion process.

## References

- [1] S.S. Medany, R.S. Elkamel, S.A. Abdel-Gawad, A.M. Fekry. A novel nano-composite CSNPs/PVP/CoONPs coating for improving corrosion resistance of Ti-6Al-4V alloy as a dental implant. *Metals*, 12 (2022) 1784. <https://doi.org/10.3390/met12111784>
- [2] P.A.B. Kuroda, F. de F. Quadros, R. Oliveira de Araújo, C.R.M. Afonso, C.R. Grandini, Effect of thermomechanical treatments on the phases, microstructure, microhardness and Young's modulus of Ti-25Ta-Zr alloys, *Materials* 12 (2019). <https://doi.org/10.3390/ma12193210>.
- [3] A. El-Ghannam, L. Starr, J. Jones, Laminin-5 coating enhances epithelial cell attachment, spreading, and hemidesmosome assembly on Ti-6Al-4V implant material in vitro, *Journal of Biomedical Materials Research: An Official Journal of The Society for Biomaterials, The Japanese Society for Biomaterials, and the Australian Society for Biomaterials* 41 (1998) 30–40.
- [4] J. Vaithilingam, E. Prina, R.D. Goodridge, R.J.M. Hague, S. Edmondson, F.R.A.J. Rose, S.D.R. Christie, Surface chemistry of Ti6Al4V components fabricated using selective laser melting for biomedical applications, *Materials Science and Engineering C* 67 (2016) 294–303. <https://doi.org/10.1016/j.msec.2016.05.054>.
- [5] C. Leyens, M. Peters, C. Leyens, M. Peters, Edited by Phase Transformations in Materials Related Titles from Wiley-VCH Magnesium Alloys and Technology Handbook of Cellular Metals, 2003.
- [6] M. Niinomi, Recent metallic materials for biomedical applications, *Metallurgical and Materials Transactions A* 33 (2002) 477–486. <https://doi.org/10.1007/s11661-002-0109-2>.
- [7] D. Banerjee, J.C. Williams, Perspectives on titanium science and technology, *Acta Materialia* 61 (2013) 844–879.
- [8] A.T. Sidambe, Biocompatibility of advanced manufactured titanium implants-A review, *Materials* 7 (2014) 8168–8188. <https://doi.org/10.3390/ma7128168>.
- [9] T. Ohtani, M. Motoki, K. Koh, K. Ohshima, Synthesis of binary copper chalcogenides by mechanical alloying, *Materials Research Bulletin* 30 (1995) 1495–1504. [https://doi.org/10.1016/0025-5408\(95\)00155-7](https://doi.org/10.1016/0025-5408(95)00155-7).
- [10] B.Y.J.J. Jacobs, M. D, J.L. Gilbert, D. Ph, R.M. Urbant, Current Concepts Review Corrosion of Metal Orthopaedic Implants \*, (1998) 268–282.
- [11] G. Lütjering, J. C. Williams, Titanium, 2nd ed., Springer, New York, (2007).
- [12] M. Wollmann, J. Kiese, L. Wagner, Properties and applications of titanium alloys in transport, *Ti 2011 - Proceedings of the 12th World Conference on Titanium 2* (2012) 837–844.
- [13] S. Nag, R. Banerjee, H.L. Fraser, Microstructural evolution and strengthening mechanisms in Ti-Nb-Zr-Ta, Ti-Mo-Zr-Fe and Ti-15Mo biocompatible alloys, *Materials Science and Engineering C* 25 (2005) 357–362. <https://doi.org/10.1016/j.msec.2004.12.013>.
- [14] M. Li, X. Min, K. Yao, F. Ye, Novel insight into the formation of  $\alpha''$ -martensite and  $\omega$ -phase with cluster structure in metastable Ti-Mo alloys, *Acta Materialia Inc.*, (2019). <https://doi.org/10.1016/j.actamat.2018.10.048>.
- [15] A. Devaraj, S. Nag, R. Srinivasan, R.E.A. Williams, S. Banerjee, R. Banerjee, H.L. Fraser, Experimental evidence of concurrent compositional and structural instabilities leading to  $\omega$  precipitation in titanium-molybdenum alloys, *Acta Materialia* 60 (2012) 596–609. <https://doi.org/10.1016/j.actamat.2011.10.008>.
- [16] A. Keshtta, M.A.-H. Gepreel, Superelasticity Evaluation of the Biocompatible Ti-17Nb-6Ta Alloy, *Journal of Healthcare Engineering* 2019 (2019). <https://doi.org/10.1155/2019/8353409>.
- [17] A. Keshtta, M.A.H. Gepreel, Effect of Sn-addition on the properties of the biomedical Ti-17Nb-6Ta alloy., *IOP Conference Series: Materials Science and Engineering* 553 (2019) 1–6. <https://doi.org/10.1088/1757-899X/553/1/012032>.
- [18] A. Keshtta, M.A.-H. Gepreel, Effect of Sn-addition on the properties of the biomedical Ti-17Nb-6Ta alloy., in: *IOP Conference Series: Materials Science and Engineering*, IOP Publishing, (2019) 12032.
- [19] A. Revathi, A.D. Borrás, A.I. Muñoz, C. Richard, G. Manivasagam, Degradation mechanisms and future challenges of titanium and its alloys for dental implant applications in oral environment, *Materials Science and Engineering C* 76 (2017) 1354–1368. <https://doi.org/10.1016/j.msec.2017.02.159>.
- [20] G. Senopati, R.A. Rahman Rashid, I. Kartika, S. Palanisamy, Recent Development of Low-Cost  $\beta$ -Ti Alloys for Biomedical Applications: A Review, *Metals* 13 (2023). <https://doi.org/10.3390/met13020194>.
- [21] P. Ou, C. Hao, J. Liu, R. He, B. Wang, J. Ruan, Cytocompatibility of Ti-xZr alloys as dental implant materials, *Journal of Materials Science:*

- Materials in Medicine 32 (2021). <https://doi.org/10.1007/s10856-021-06522-w>.
- [22] A. Keshtta, A.H. Awad, H.A. Aly, G.A. Elnaser, T. Elsarag, Effects of Zr Addition on Magnetic Susceptibility of Novel Biocompatible Ti-10Mo-(x) Zr Alloys for Biomedical Implants., 4 (2024) 9–13.
- [23] Q. Wang, C. Dong, P.K. Liaw, Structural Stabilities of  $\beta$ -Ti Alloys Studied Using a New Mo Equivalent Derived from  $[\beta/(\alpha + \beta)]$  Phase-Boundary Slopes, Metallurgical and Materials Transactions A: Physical Metallurgy and Materials Science 46 (2015) 3440–3447. <https://doi.org/10.1007/s11661-015-2923-3>.
- [24] D. Kuroda, M. Niinomi, M. Morinaga, Y. Kato, T. Yashiro, Design and mechanical properties of new  $\beta$  type titanium alloys for implant materials, Materials Science and Engineering A 243 (1998) 244–249. [https://doi.org/10.1016/s0921-5093\(97\)00808-3](https://doi.org/10.1016/s0921-5093(97)00808-3).
- [25] W. Elmay, P. Laheurte, A. Eberhardt, B. Bolle, T. Gloriant, E. Patoor, F. Prima, D. Laille, P. Castany, M. Wary, Stability and elastic properties of Ti-alloys for biomedical application designed with electronic parameters, EPJ Web of Conferences 6 (2010) 6. <https://doi.org/10.1051/epjconf/20100629002>.
- [26] J.H.C. Lin, Y.H. Fu, Y.C. Chen, Y.P. Peng, C.P. Ju, Solution treatment-delayed zirconium-strengthening behavior in Ti-7.5Mo-xZr alloy system, Materials Research Express 5 (2018). <https://doi.org/10.1088/2053-1591/aaa6e4>.
- [27] D.R.N. Correa, P.A.B. Kuroda, M.L. Lourenço, C.J.C. Fernandes, M.A.R. Buzalaf, W.F. Zambuzzi, C.R. Grandini, Development of Ti-15Zr-Mo alloys for applying as implantable biomedical devices, Journal of Alloys and Compounds 749 (2018) 163–171. <https://doi.org/10.1016/j.jallcom.2018.03.308>.
- [28] C. Suwanpreecha, S. Songkuea, P. Wangjina, M. Tange, W. Pongsaksawad, A. Manonukul, Effect of Mo Additions on the Physical, Mechanical and Corrosion Properties of Commercially Pure Ti Fabricated by Metal Injection Moulding, Metals and Materials International 29 (2023) 3298–3316. <https://doi.org/10.1007/s12540-023-01454-2>.
- [29] A.P. Ramos, W.B. de Castro, J.D. Costa, R.A.C. de Santana, Influence of zirconium percentage on microhardness and corrosion resistance of Ti50 Ni50-xZrx shape memory alloys, Materials Research 22 (2019). <https://doi.org/10.1590/1980-5373-MR-2018-0604>.
- [30] A. Sotniczuk, W. Chromiński, D. Kalita, H. Garbacz, C. Xie, J. Tang, B. Dou, M. Pisarek, A. Baron-Wiecheć, Ł. Kurpaska, F. Sun, K. Ogle, Effect of Zr addition on the corrosion resistance of Ti-Mo alloy in the H<sub>2</sub>O<sub>2</sub>-containing inflammatory environment, Applied Surface Science 681 (2025). <https://doi.org/10.1016/j.apsusc.2024.161518>.
- [31] Y. Huang, B. Cai, D. Yuan, Z. Guo, Construction of porous micro/nano structures on the surface of Ti-Mo-Zr alloys by anodic oxidation for biomedical application, Journal of Materials Research and Technology 30 (2024) 2986–2998. [doi.org/10.1016/j.jmrt.2024.04.046](https://doi.org/10.1016/j.jmrt.2024.04.046).
- [32] A.H. Awad, H.A. El-hofy, A. Chiba, M.A. Gepreel, Robust mechanical properties and corrosion resistance of new low-cost hot-forged and aged  $\beta$ -type Ti-14Mn-(x)Zr alloys, Journal of Alloys and Compounds 904 (2022) 164098. <https://doi.org/10.1016/j.jallcom.2022.164098>.
- [33] H. Wu, T. Wang, X. Liu, N. Lin, X. Liu, Z. He, Z. Wang, Fabrication and corrosion resistance of the Ti-rich alloyed layer on the surface of NiTi alloys, International Journal of Electrochemical Science 12 (2017) 2376–2388. <https://doi.org/10.20964/2017.03.51>.
- [34] Y.-L. Zhou, D.-M. Luo, Corrosion behavior of Ti-Mo alloys cold rolled and heat treated, Journal of Alloys and Compounds 509 (2011) 6267–6272. <https://doi.org/https://doi.org/10.1016/j.jallcom.2011.03.045>.
- [35] R.E. Hammam, E.M. Safwat, S.A. Abdelgwad, M. Shoeib, S. EL-Hadad, Influence of anodization conditions on deposition of hydroxyapatite on  $\alpha/\beta$  Ti alloys for osseointegration: Atomic force microscopy analysis, Transactions of Nonferrous Metals Society of China (English Edition) 34 (2024) 3629–3649. [https://doi.org/10.1016/S1003-6326\(24\)66630-6](https://doi.org/10.1016/S1003-6326(24)66630-6).
- [36] E.M. Safwat, S.A. Abdel-Gawad, M.A. Shoeib, S. El-Hadad, Electrochemical anodization of cast titanium alloys in oxalic acid for biomedical applications, Frontiers of Chemical Science and Engineering 18 (2024) 1–12. <https://doi.org/10.1007/s11705-023-2368-y>.
- [37] A.W. Abdelghany, Awad, Ahmed H., Modar Saood, Hayam A. Aly, The Role of Mo and Zr Additions in Enhancing the Behavior of New Ti-Mo Alloys for Implant Materials, Metals and Materials International (2014).
- [38] Y.L. Zhou, D.M. Luo, Microstructures and mechanical properties of Ti-Mo alloys cold-rolled and heat treated, Materials Characterization 62 (2011) 931–937. <https://doi.org/10.1016/j.matchar.2011.07.010>